

Structural Changes in Surfactant-Modified Sorbents During Furnace Injection

A calcium hydroxide $[\text{Ca}(\text{OH})_2]$ sorbent modified by the addition of calcium lignosulfonate has recently been developed for use in the Environmental Protection Agency's limestone injection multistage burner process. The increased reactivity with sulfur dioxide (SO_2) displayed by this modified sorbent has been shown to be caused, in part, by its decreased particle (agglomerate) size compared to conventional $\text{Ca}(\text{OH})_2$. Subsequent work has shown that surfactant-modified $\text{Ca}(\text{OH})_2$ also undergoes significantly different structural changes during furnace injection. For a given reactor temperature and residence time, the modified sorbent calcines to a greater extent than unmodified sorbent. It also loses surface area more slowly, and retains more of its porosity, suggesting that it sinters more slowly than conventional sorbent. Therefore, in addition to reducing the particle size of $\text{Ca}(\text{OH})_2$ in some applications, calcium lignosulfonate also appears to cause the water of hydration to be bound less tightly, and to inhibit one or more of the diffusion mechanisms responsible for the process of sintering.

David A. Kirchgessner
United States Environmental
Protection Agency
Air and Energy Engineering
Research Laboratory
Research Triangle Park, NC 27711

Wojciech Jozewicz
Acurex Corporation
Research Triangle Park, NC 27709

Introduction

The Environmental Protection Agency's LIMB (limestone injection multistage burner) process is designed to reduce SO_2 emissions from coal-fired boilers through the injection of a dry, calcium-based sorbent into the furnace at about $1,230^\circ\text{C}$, while reductions in NO_x are achieved by delaying the mixing of fuel and air through the multistage burner. A lengthy testing program has shown that, of the commercially available calcium-based sorbents, calcium hydroxide, $\text{Ca}(\text{OH})_2$, produces the highest levels of SO_2 capture (Overmoe et al., 1985; Beittel et al., 1985; Bortz and Flament, 1985; Slaughter et al., 1985).

Recent efforts to improve the capture of SO_2 by commercial $\text{Ca}(\text{OH})_2$ involve the addition of calcium lignosulfonate to the water of hydration to produce $\text{Ca}(\text{OH})_2$ that has a smaller particle size, and a 15–20% higher reactivity with SO_2 relative to conventional $\text{Ca}(\text{OH})_2$ (Kirchgessner and Lorrain, 1987). The effect of smaller particle size on reactivity has been widely documented (McCarthy et al., 1986; Borgwardt and Bruce, 1986a; Cole et al., 1986) and is of the order -0.20 to -0.35 (Ishihara et al., 1975; Gullett and Blom, 1987; Gullett and Kramlich, 1987). The enhanced reactivity noted at laboratory scale by

Kirchgessner and Lorrain is partially, but not fully, explained by particle size reduction in the modified hydrate.

Surface area and pore structure of the calcined sorbent are also important determinants of reactivity. The relationship of surface area of the calcined sorbent to its ultimate level of sulfation has been widely documented (Newton et al., 1985; Harrison et al., 1985; Cole et al., 1985; Beittel et al., 1985; Slaughter et al., 1985; Borgwardt and Bruce, 1986b). Borgwardt and Bruce (1986b) have quantified the relationship in noting that the reactivity increases with the square of the BET surface area of the calcine over the range $2\text{--}63\text{ m}^2/\text{g}$. The importance of porosity in the CaO was noted by Hartman et al. (1978). Aside from the effect of particle size, surface area and porosity are, therefore, the logical parameters to examine in determining the source of enhanced reactivity in modified $\text{Ca}(\text{OH})_2$.

The purpose of this research is to determine the mechanism(s), other than particle size reduction, by which lignosulfonate modification increases the reactivity of $\text{Ca}(\text{OH})_2$ with SO_2 . Experiments were conducted in a $700\text{--}1,000^\circ\text{C}$ flow reactor. SO_2 was omitted in order to decouple the calcination and sintering processes from the sulfation process. It was observed that the modified $\text{Ca}(\text{OH})_2$ calcined more quickly, and retained more of its original surface area and porosity than the conventional $\text{Ca}(\text{OH})_2$.

Correspondence concerning this paper should be addressed to D. A. Kirchgessner.

Table 1. Elemental Analysis of Longview Limestone

Component	ppm
Ca	353,000
Mg	6,200
Si	2,200
Al	689
Fe	657
Mn	24
Na	—

Experimental System

Materials

The parent material for the $\text{Ca}(\text{OH})_2$ used in this study is a commercial CaO obtained from the Longview Lime Division of Dravo Lime Co., Saginaw, Alabama. A chemical analysis of the carbonate from which the CaO was derived is given in Table 1. These elemental concentrations are not considered exceptional among commercial stones.

The additive used in the modified $\text{Ca}(\text{OH})_2$ is calcium lignosulfonate. Specifically, it is a partially desugared variety in the form of a water-soluble dry powder available from Georgia Pacific Corp. under the trade name Lignosite. The material is discussed elsewhere by Grayson (1983) under the category Anionic Surfactants, and by Rosen (1978) under Dispersants.

Hydration

Hydrates are produced in a steam-jacketed Ross ribbon blender. To produce conventional $\text{Ca}(\text{OH})_2$, the blender is loaded with 6.8 kg pulverized CaO and allowed to reach a temperature of 30–50°C. A total of 3.7 kg water is then added at a constant rate for 40 min. The blender is run for an additional 20 min while the heat of reaction drives off excess water, leaving a dry $\text{Ca}(\text{OH})_2$ product [$\text{DH-Ca}(\text{OH})_2$]. The procedure for producing surfactant-modified $\text{Ca}(\text{OH})_2$ [$\text{SM-Ca}(\text{OH})_2$] is identical except that the 3.7 kg water contains 102 g Lignosite. This yields a $\text{Ca}(\text{OH})_2$ product containing approximately 1 mass % of calcium lignosulfonate, the amount shown by Kirchgessner and Lorrain (1987) to be optimal for enhancement of SO_2 capture.

Reactors

The electrically heated, isothermal flow reactor into which the hydrates are injected for structural studies is shown in Figure 1. The reaction chamber consists of two concentric, 3.35 m long quartz tubes heated by three Lindberg tube furnaces. The inner tube has a 15 mm ID, and the outer tube has a 50.8 mm OD. Premixed gases enter the reactor at the bottom of the annulus between the inner and outer tubes and are heated as they move upward. At the top of the reactor they enter the inner tube with the sorbent and move downward through the reaction zone. Gases and solids exit the reactor through an air-cooled heat exchanger that quenches the reactant stream to approximately 280°C. Solids are captured in a cyclone followed by a glass-fiber filter. Sorbent is fed from a fluidized bed feed tube through 1.9 mm ID syringe tubing. The reactor is operated at nominal temperatures of 700–1,000°C, and nominal residence times of 0.6–2.0 s. Residence time is adjusted by varying gas flow, at standard temperature and pressure (25°C, 760 mm Hg [101 kPa]) from 25.54 to 5.86 L/min. Gas composition is 95 vol. % N_2 and 5 vol. % O_2 to be compatible with earlier experiments. SO_2 is omit-

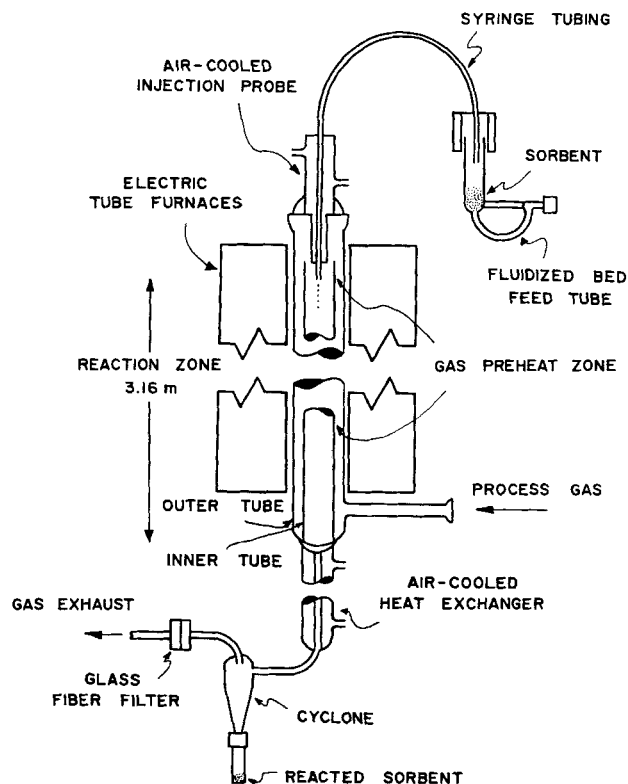


Figure 1. Isothermal flow reactor.

ted in this case because the objective of the research is to observe calcination and sintering behavior without the additional complication of sulfation, which would effectively mask the surface area and pore structure changes of interest through product layer buildup and pore plugging. Due to variability in the reactor system, selected samples are replicated until standard deviation falls to less than 10% of the mean.

The differential reactor shown in Figure 2 has been used by Borgwardt (1988) to determine the maximum calcined surface areas of a series of calcium hydroxides, and is used in this study for making the same determination on modified hydroxides. The reactor consists of two concentric quartz glass tubes, 3 cm ID and 2 cm ID, each 95 cm long. Gases enter the outer annulus at the bottom, are preheated as they move upward, and then flow downward to the reaction zone. The 1.4 cm ID quartz glass sample holder is positioned in the approximate center of the reactor. The hydroxide sample is supported on a bed of quartz glass wool in the sample holder so that heated gases pass through it. The entire reactor is supported in a Lindberg tube furnace.

CaO is prepared from 25 mg samples of $\text{Ca}(\text{OH})_2$ inserted into the 700°C reactor with an N_2 flow of 20 L/min. At the conclusion of the 5 min calcination period, the sample is cooled under flowing N_2 and transferred to a BET flask. Fourteen of these runs are composited for a single analysis of surface area. In this well-controlled reactor, standard deviations of as little as 3 to 6% of the mean are achieved.

Analysis

The degree of dehydration in samples is determined using a DuPont 951 thermogravimetric analyzer. Specific surface area, porosity, and pore size distribution are measured by N_2 adsorp-

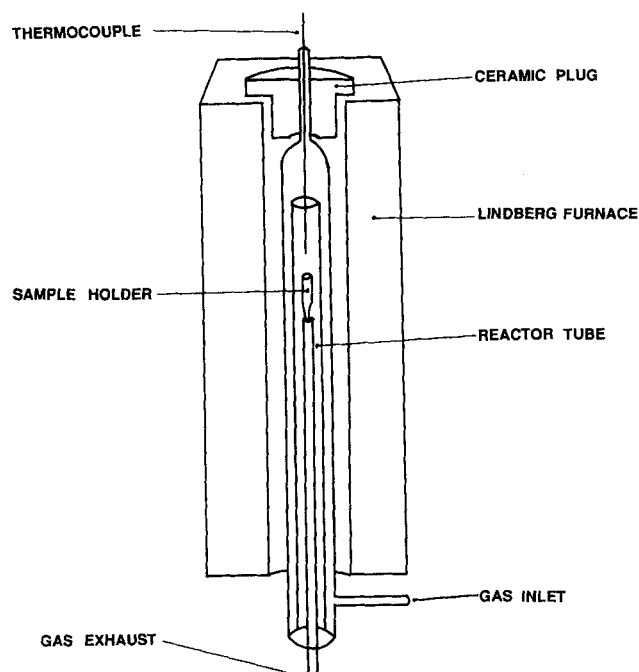


Figure 2. Differential reactor.

tion/desorption in a Micromeritics Digisorb 2600 autoanalyzer. Measurement error on both machines is less than $\pm 1\%$.

Results and Discussion

Surface area

Figure 3 illustrates the deterioration of surface area over time and at increasing temperatures, as a result of sintering in the CaO derived from both modified and unmodified Ca(OH)_2 . Since surface area of the raw Ca(OH)_2 is approximately $15\text{--}20\text{ m}^2/\text{g}$, it is apparent that much higher surface areas initially develop during calcination and have begun to decay by 0.6 s. It can be seen at all three temperatures that the CaO derived from surfactant-modified Ca(OH)_2 (SM-CaO) loses surface area more slowly than the CaO derived from unmodified Ca(OH)_2 (DH-CaO), suggesting that sintering proceeds more slowly in the former sorbent. Figure 3 also shows the enhanced effects of sintering at higher temperatures, although SM-CaO retains its advantage in the range of 700 to $1,000^\circ\text{C}$.

Choice of the original calcined surface areas for both the modified and unmodified oxides is critical to this interpretation. Borgwardt (1988) has experimentally determined the maximum calcined surface areas, under optimal conditions, for a series of calcium hydroxides that have a mean value of $76.7\text{ m}^2/\text{g}$ and a standard deviation of 2.4. The associated porosity is 0.40. Using the same reactor and reaction conditions, it has been determined in this study that the maximum calcined surface area of the modified hydroxide is $76.2\text{ m}^2/\text{g}$ with a standard deviation of 4.6. This is regarded as being essentially identical to the unmodified hydroxide. These values are used to interpret the data in Figures 3 and 10.

Pore structure

Further evidence of the difference in sintering rates between SM-CaO and DH-CaO is found in the evolution of the

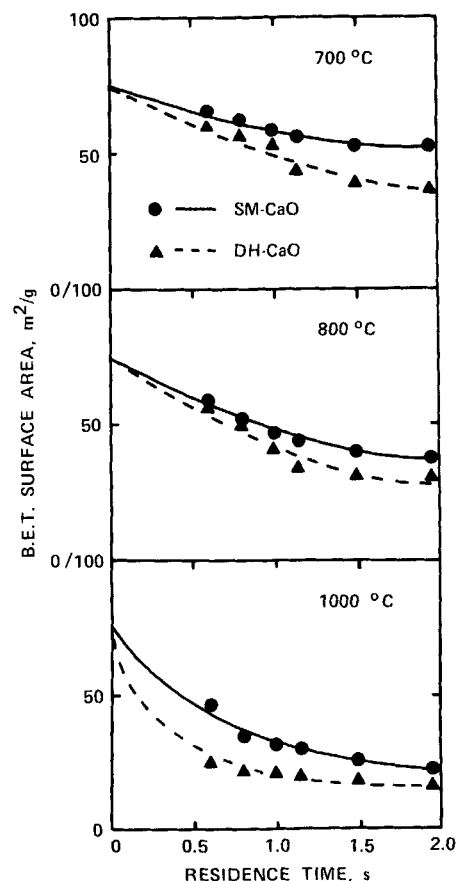


Figure 3. Surface area reduction in SM-CaO and DH-CaO as a function of time and temperature.

respective pore structures over time. Figure 4 shows the change in porosity over time for both sorbents as a function of temperature. As time and temperature conditions become more severe the difference between sorbents becomes more pronounced, with SM-CaO retaining more of its original porosity in all cases. At

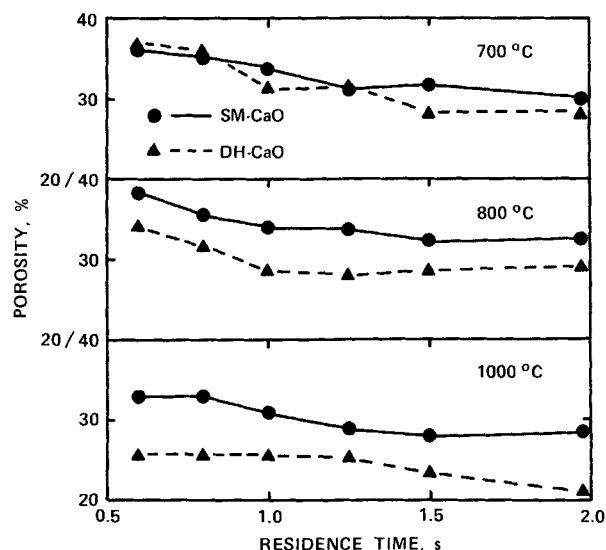


Figure 4. Porosity reduction in SM-CaO and DH-CaO as a function of time and temperature.

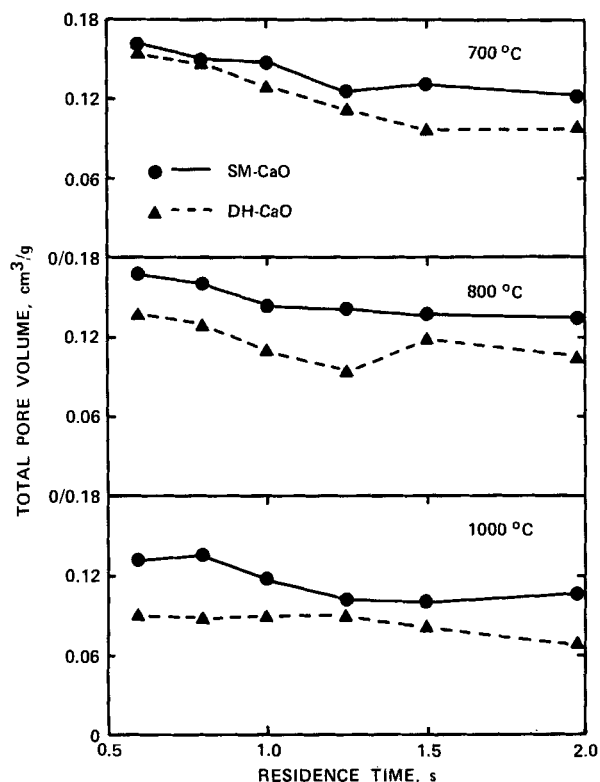


Figure 5. Pore volume reduction in SM-CaO and DH-CaO as a function of time and temperature.

the extreme sintering conditions of 1,000°C for 2 s, SM-CaO retains a porosity of 29% while that of DH-CaO has been reduced to 21%. It should be noted that both sorbents, at all conditions, have lost a significant amount of their original surface area, suggesting that the sintering process is well along. A theoretical original porosity of 49% has been calculated for $\text{Ca}(\text{OH})_2$ -derived CaO. Thus, even under the mildest conditions of 700°C for 0.6 s, both sorbents have lost 30% of their original porosity through sintering. Figure 5 presents the data in terms of actual pore volume.

Porosity data, in their raw form, are obtained as a function of pore size. Therefore, a plot of cumulative pore volume vs. pore size can be produced, and a median pore size can be identified below which 50% of the volume resides. Figure 6 shows the median pore sizes for each experimental condition of time and temperature. Since a significant portion of the sintering process involves filling pores, with the smallest being filled first, the expected behavior is for the median pore size to become larger at more severe conditions where sintering is more advanced. Figure 6 reflects this prediction quite well. In general, it can be seen that at a given residence time, higher temperatures yield larger median pore sizes. Similarly, at a given temperature increasing residence times produce larger median pores. As with surface area and porosity, the differences in median pore sizes between SM-CaO and DH-CaO become more pronounced at higher temperatures.

Figure 7 describes the sintering process from another perspective. Pore volume, normalized with respect to maximum pore volume available ($0.21 \text{ cm}^3/\text{g}$), is plotted vs. residence time for three pore size ranges. In this fashion one can observe the rate of

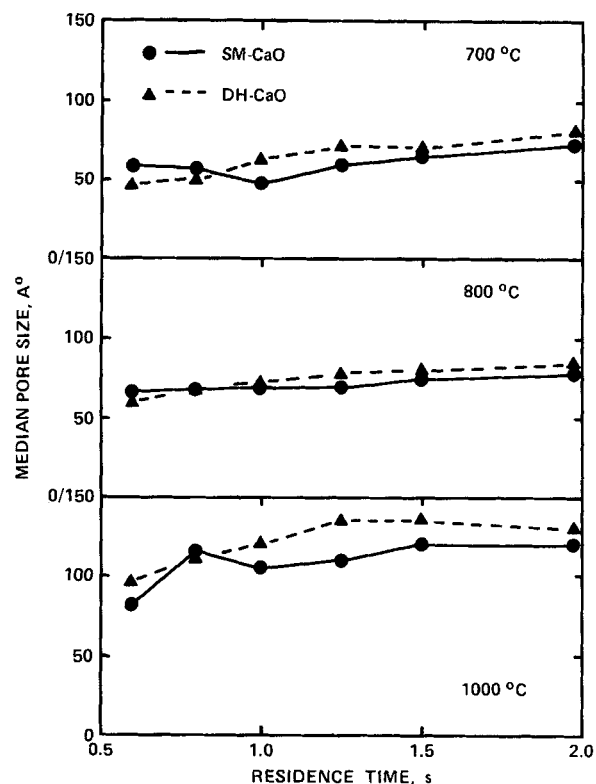


Figure 6. Increase of median pore size in SM-CaO and DH-CaO as a function of time and temperature.

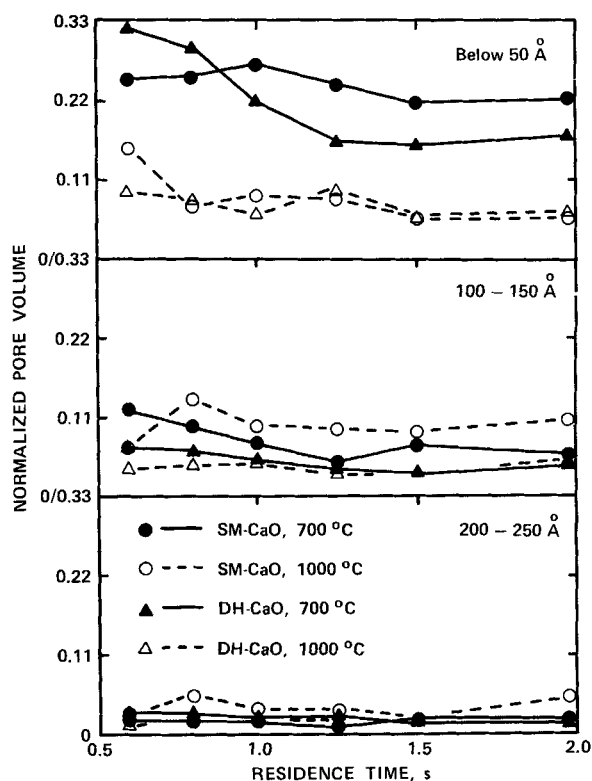


Figure 7. Changes in normalized pore volume as a function of time, temperature, and pore size range.

annihilation of pores from finer size ranges (below 50 Å [5 nm]) where the most dramatic changes with time and temperature occur. Pore volume in the range below 50 Å decreases very quickly at 700°C and has reached an apparently stable level by 1.5 s. The SM-CaO retains much more pore volume in this size range than DH-CaO. The 1,000°C data for this range of pores show little difference between sorbents or over time. This suggests that the finest pore structure, at these conditions, has been sintered down to a relatively stable level by 0.8 s.

Pore volume in the range 100–150 Å (10–15 nm) does not show the dramatic changes observed in the finer sizes, but the SM-CaO clearly retains more pore volume than DH-CaO for nearly all experimental conditions. Behavior of pore volume in the 200–250 Å (20–25 nm) range, as well as in the 250–300 Å (25–30 nm) and above 300 Å ranges not shown in Figure 7, is essentially constant for all experimental conditions and sorbents. Increases in pore volume for larger size ranges are not seen because, during this stage of sintering, pores are being filled rather than being assimilated by larger pores.

Briefly, the respective differences in surface area deterioration, and in pore structure evolution, suggest that SM-CaO is more resistant to sintering than is DH-CaO. Further, it appears that most of the observed differences become more pronounced as the experimental conditions become more severe. A final observation is that the largest changes in both surface area and pore structure appear to be complete by 1.5 s, suggesting that sintering has reached the end of the stage in which porosity reduction occurs.

Rate of dehydration

Since it has previously been shown that the sintering of CaO is catalyzed by H₂O (Anderson et al., 1965), it was believed that differences in the rates of water loss for modified and unmodified Ca(OH)₂ may explain the differences in the rates of surface area loss and in pore structure. Temperature profiles recorded during the hydration process show a delay in temperature rise when hydrating with surfactants, due to the difficulty of achieving complete hydration with a material containing a hydrophobic component. In addition, preliminary TGA results suggested that SM-CaO loses chemically bound water from 247 to 417°C, while DH-CaO loses water from 270 to 435°C. Thus the modified Ca(OH)₂ was expected to dehydrate more easily, and to have less water available at any point in time to catalyze sintering. Figure 8 shows the amount of hydration water lost over times from 0.6 to 2.0 s at temperatures from 700 to 1,000°C. As expected, the water loss from modified Ca(OH)₂ at any condition is greater than the loss from unmodified Ca(OH)₂ at similar conditions. The difference in rate of water loss, however, appears to take place before 0.6 s. From that point on, the data sets for both sorbents are essentially parallel. This contrasts to the data in Figure 3 for 700 and 800°C in that the surface area differences between sorbents do not become pronounced until after 0.6 s. Since the time frames for the difference in rate of water loss and the difference in rate of surface area loss are not the same, it is doubtful that water loss can be regarded as a causative factor at 700 and 800°C. It may, however, provide a partial explanation of the 1,000°C data set in Figure 3.

Diffusion

Since the difference in amounts of water available to catalyze sintering does not appear to fully explain the data, another

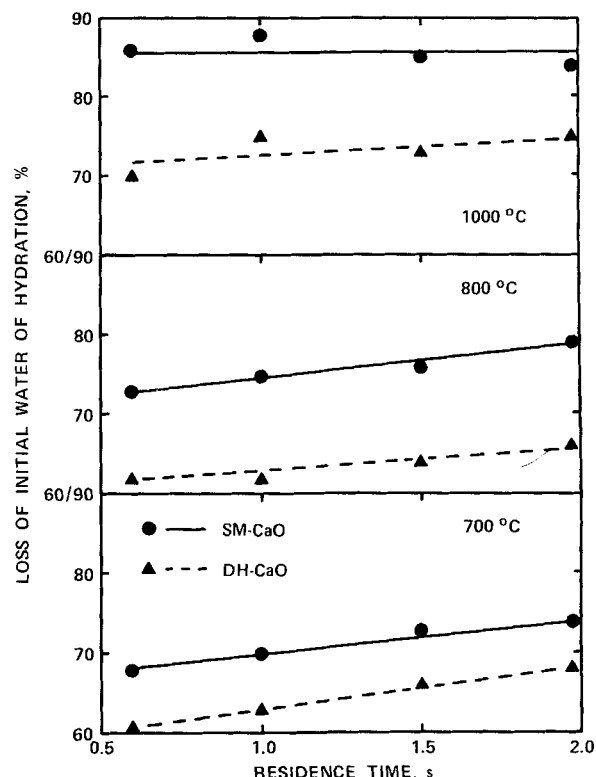


Figure 8. Rate of dehydration in SM-CaO and DH-CaO as a function of temperature.

mechanism must be considered by which sintering in SM-CaO is inhibited. It is suggested that the presence of calcium lignosulfonate, or its residue, retards the diffusion mechanism by which sintering proceeds in the SM-CaO.

Schmalzried (1974) offers a brief description of the sintering process that lends itself well to this discussion. The process is graphically summarized in Figure 9, which shows the variation over time of the three primary variables: surface area, porosity, and grain size. In stage I, surface area is reduced through the growth of necks between adjacent particles or grains, and the consequent rounding of pores located at the intersection of grain boundaries. During this stage, diffusion may proceed by the mechanisms of plastic flow, lattice diffusion, grain boundary diffusion, or surface diffusion.

During stage II, surface area is reduced further as pores are filled. The chemical potential of a substance is less at the negatively curved surface of a pore than at the planar grain boundaries, so the resulting gradient will cause the transfer of material from grain boundaries and surfaces to the pores. This is also the reason for the smallest pores being filled first. Burke et al. (1980) refer to stage II as densification because of the decrease in porosity. The transport processes during this stage are both grain boundary and volume diffusion.

Stage III is characterized by the growth of the grains themselves through a process Burke et al. (1980) call coarsening. Pore annihilation along grain boundaries ceases if and when grain boundary mobility exceeds pore mobility, at which point pores are left behind in what becomes the interiors of grains. Pores within grains can continue to coalesce through a process of parasitic pore growth, but no net change in porosity occurs as a result of this process.

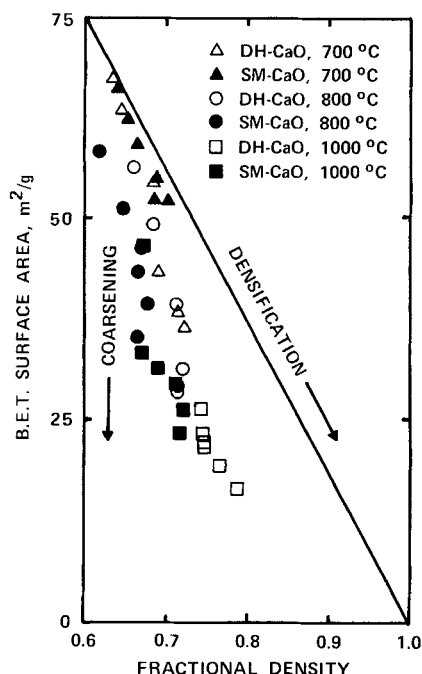


Figure 9. Reduction in surface area with increasing density in SM-CaO and DH-CaO.

The three stages of sintering are described as though they occur in series and, at the molecular level, they do. Within a particle or an aggregate of particles of various sizes, however, any of the three stages may be present at a given time as the reaction front moves from the surface to the center of the mass. For this reason, analyses intended to identify the stage of sintering that a material has achieved will generally show properties characteristic of more than one stage, or of intermediate stages. That situation is shown in Figure 10 where the data from this work are plotted on a graph of surface area vs. fractional density ($1 - \text{porosity}$) in the fashion of Burke et al. (1980). If all surface area reduction occurs through grain coarsening the data would appear as a trend parallel to the surface area axis. If surface area is lost, instead, through pore filling, the data would appear as a trend parallel to the diagonal line labeled Densification. The locus of these two lines has a surface area of $75 \text{ m}^2/\text{g}$ and a fractional density of 0.6 (porosity = 0.4) based on the maximum calcined values determined experimentally by Borgwardt (1988). The data in fact fall between these extremes, suggesting that under all experimental conditions at least some material has progressed to stage III. Higher temperatures and longer times produce data points in Figure 10 that are the lowest in surface area and closest to the coarsening trajectory, suggesting the most advanced stage of sintering.

Burke et al. (1980) have studied the effect of magnesium oxide (MgO) on the sintering of aluminum oxide (Al_2O_3). It had been recognized that the presence of MgO allows sintering to proceed to theoretical density, and their objective was to determine the mechanism involved. They concluded that the presence of MgO at grain boundaries reduces grain boundary mobility, perhaps through the phenomenon of solvent drag, thus delaying the onset of discontinuous grain growth and the entrapment of residual pores within grains. They noted also that the presence

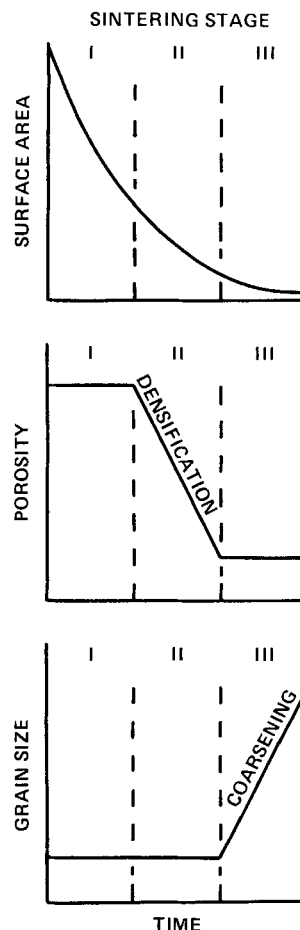


Figure 10. Changes in surface area, porosity, and grain size during sintering.

of MgO reduced the rate of surface area loss, porosity loss, and possibly grain growth.

Because of the large size of the hydrated lignosulfonate molecule (ca. 100 \AA [10 nm]), it is believed to be located at the grain boundaries and surfaces of the $\text{Ca}(\text{OH})_2$ rather than within the crystal structure. In this position the lignosulfonate, or its residue after calcination, is thought to be capable of exerting an influence similar to that of the MgO on Al_2O_3 . Since it has been shown that the CaO in this study has been sintered to the point of grain coarsening (stage III), there has been ample time for the inhibition of surface area and porosity reduction to express itself. The inhibition of grain growth cannot be shown with the available data.

Conclusions

A previous study has shown that in certain applications the addition of calcium lignosulfonate during the production of $\text{Ca}(\text{OH})_2$ yields a sorbent with a reduced tendency to agglomerate and an increased reactivity with SO_2 . The research presented here shows that lignosulfonate modification also has the ability to inhibit the rate of sintering in $\text{Ca}(\text{OH})_2$ injected into the hot zone of a reactor or boiler. This inhibition expresses itself in higher surface areas and porosities, and lower median pore sizes in sintered modified sorbents. The higher surface areas and porosities available during the 1.0 to 1.5 s time frame normally

available for sulfation during boiler injection, will allow modified sorbents to react with SO_2 to a greater extent than unmodified sorbents.

Acknowledgment

This research was supported by the U.S. Environmental Protection Agency's Air and Energy Engineering Research Laboratory. The authors wish to acknowledge the assistance of Peter Blades, Kevin Bruce, and Laura Beach of Acurex Corp., and George Gillis of EPA.

Literature Cited

- Anderson, P. J., R. F. Horlock, and R. G. Avery, "Some Effects of Water Vapour During the Preparation and Calcination of Oxide Powders," *Proc. Brit. Ceram. Soc.*, **3**, 33 (1965).
- Beittel, R., J. P. Gooch, E. B. Dismukes, and L. J. Muzio, "Studies of Sorbent Calcination and SO_2 -Sorbent Reactions in a Pilot-Scale Furnace," *Proc. 1st Joint Symp. Dry SO_2 and Simul. SO_2/NO_x Control Technol. 1*, EPA-600/9-85-020a (NTIS PB85-232353), 16-1 (July, 1985).
- Borgwardt, R. H., "Sintering of Nascent Calcium Oxide," *Chem. Eng. Sci.*, **44**, 53 (1988).
- Borgwardt, R. H., and K. R. Bruce, "EPA Study of Hydroxide Reactivity in a Differential Reactor," *Proc. 1986 Joint Symp. Dry SO_2 and Simul. SO_2/NO_x Control Technol. 1*, EPA-600/9-86-029a (NTIS PB87-120465), p. 15-1 (Oct., 1986a).
- , "Effect of Specific Surface Area on the Reactivity of CaO with SO_2 ," *AIChE J.*, **32**, 239 (1986b).
- Bortz, S., and P. Flament, "Recent IFRF Fundamental and Pilot-Scale Studies on the Direct Sorbent Injection Process," *Proc. 1st Joint Symp. Dry SO_2 and Simul. SO_2/NO_x Control Technol. 1*, EPA-600/9-85-020a (NTIS PB85-232353), p. 17-1 (July, 1985).
- Burke, J. E., K. W. Lay, and S. Prochazka, "The Effect of MgO on the Mobility of Grain Boundaries and Pores in Aluminum Oxides," *Sintering Processes*, G. C. Kuczynski, ed., Plenum, New York, 417 (1980).
- Cole, J. A., J. C. Kramlich, W. R. Seeker, and M. P. Heap, "Activation and Reactivity of Calcareous Sorbents Toward Sulfur Dioxide," *Env. Sci. Technol.*, **19**, 1065 (1985).
- Cole, J. A., J. C. Kramlich, W. R. Seeker, G. D. Silcox, G. H. Newton, D. J. Harrison, and D. W. Pershing, "Fundamental Studies of Sorbent Reactivity in Isothermal Reactors," *Proc. 1986 Joint Symp. Dry SO_2 and Simul. SO_2/NO_x Control Technol. 1*, EPA-600/9-86-029a (NTIS PB87-120465), 16-1 (Oct., 1986).
- Grayson, M., ed., *Kirk-Othmer Encyclopedia of Chemical Technology*, Wiley, New York (1983).
- Gullett, B. K., and J. A. Blom, "Calcium Hydroxide and Calcium Carbonate Particle Size Effects on Reactivity with Sulfur Dioxide," *Reac. Solids*, **3**, 337 (1987).
- Gullett, B. K., and J. C. Kramlich, "Fundamental Processes Involved in SO_2 Capture by Calcium-Based Sorbents," *Proc. 4th Ann. Pitts. Coal Conf.*, (Sept.-Oct., 1987).
- Harrison, D. J., G. H. Newton, and D. W. Pershing, "Calcination of Calcium-Based Sorbents for Control of SO_2 Emissions from Coal-Fired Boilers," Western States Sect., Combust. Inst. Fall Meet., Davis, CA (Oct., 1985).
- Hartman, M., J. Pata, and R. W. Coughlin, "Influence of Porosity of Calcium Carbonates on Their Reactivity with Sulfur Dioxide," *Ind. Eng. Chem. Process Des. Dev.*, **17**, 411 (1978).
- Ishihara, Y., C. Asakawa, and H. Fukuzawa, *Nenryo Kyokaishi (J. Fuel Soc. Japan)*, **54**, 175 (1975).
- Kirchgesner, D. A., and J. M. Lorrain, "Lignosulfonate-Modified Calcium Hydroxide for Sulfur Dioxide Control," *Ind. Eng. Chem. Res.*, **26**, 2397 (1987).
- McCarthy, J. M., S. L. Chen, J. C. Kramlich, W. R. Seeker, and D. W. Pershing, "Reactivity of Atmospheric and Pressure Hydrated Sorbents for SO_2 Control," *Proc. 1986 Joint Symp. Dry SO_2 and Simul. SO_2/NO_x Control Technol. 1*, EPA-600/9-86-029a (NTIS PB87-120465), 10-1 (Oct., 1986).
- Newton, G. H., D. J. Harrison, G. D. Silcox, and D. W. Pershing, "Control of SO_x Emissions by In-Furnace Sorbent Injection: Carbonates vs. Hydrates," *AIChE Ann. Meet.*, Chicago (Nov., 1985).
- Overmoe, B. J., S. L. Chen, L. Ho, W. R. Seeker, M. P. Heap, and D. W. Pershing, "Boiler Simulator Studies on Sorbent Utilization for SO_2 Control," *Proc. 1st Joint Symp. Dry SO_2 and Simul. SO_2/NO_x Control Technol. 1*, EPA-600/9-85-020a (NTIS PB85-232353), 15-1 (July, 1985).
- Rosen, M. J., *Surfactants and Interfacial Phenomena*, Wiley, New York (1978).
- Schmalzried, H., *Solid State Reactions*, Academic Press, New York (1974).
- Slaughter, D. M., G. D. Silcox, P. M. Lemieux, G. H. Newton, and D. W. Pershing, "Bench-Scale Evaluation of Sulfur Sorbent Reactions," *Proc. 1st Joint Symp. Dry SO_2 and Simul. SO_2/NO_x Control Technol. 1*, EPA-600/9-85-020a (NTIS PB85-232353), 11-1 (July, 1985).

Manuscript received Feb. 2, 1988, and revision received Nov. 9, 1988.